

Analytical Treatment of Fragmentation-Diffusion Population Balance

M. Kostoglou

Chemical Process Engineering Research Institute, P.O. Box 1517, 54006 Thessaloniki, Greece

Anastasios J. Karabelas

Chemical Process Engineering Research Institute, P.O. Box 1517, 54006 Thessaloniki, Greece
and

Dept. of Chemical Engineering, Univ. Box 455, Aristotle University of Thessaloniki, GR 54124 Thessaloniki, Greece

DOI 10.1002/aic.10286

Published online in Wiley InterScience (www.interscience.wiley.com).

The quest for advanced models to realistically simulate various processes involving populations of “particles” (aerosols, dispersions of all kinds, minerals, cultures of microorganisms) necessitates the extension of the classical population balance formulation, which is of zero dimension (lumped) in external and one-dimensional (1-D) (single particle-characterization variable) in internal coordinate space, to more dimensions in both spaces. In order to contribute in this direction, this work is focused on a spatially distributed fragmentation equation, the spatial nonuniformity being governed by a diffusion mechanism and by deposition of particles on solid boundaries. The combined effect of diffusion and fragmentation on the particle-size distribution is of interest here. The linear form of the fragmentation-diffusion equation allows a convenient analytical manipulation, based on decomposition of solutions in spatial and temporal modes. Generalized solutions are derived for the above equation for arbitrary spatial domains, fragmentation functions, deposition rates and particle sources. The above approach can be combined with the well-known approaches for the numerical solution of the lumped fragmentation equation to derive solutions for the fragmentation-diffusion equation under arbitrary conditions. This study, as a first step, is restricted to obtaining explicit results for some rather simple cases, for example, power law fragmentation and deposition rates, fragmentation in equal sizes and simple shapes of the domain under consideration. © 2004 American Institute of Chemical Engineers AIChE J, 50: 1746–1759, 2004

Introduction

The population balance formulation is based on a macroscopic equation which describes the evolution of a population of “objects”. Each object can be described by a set of coordi-

nates including the three space coordinates. In recent decades, population balance analysis has proven to be an important tool for the engineering discipline, capable of tackling a broad range of problems. Typical examples are the kinetics of polymerization (Kiparissides, 1996), crystallization (Randolph and Larson, 1971), and precipitation phenomena (Sönnel and Gar-side, 1992), aerosol dynamics (Friedlander, 1977) and dynamics of cellular populations (Nielsen and Villadsen, 1994). These examples are selected to stress the particular importance of the population balances in chemical engineering, as they are necessary for the proper design of polymerization and aerosol

Correspondence concerning this article should be addressed to A. J. Karabelas at karabaj@alexandros.cperi.certh.gr

Current address of M. Kostoglou: Division of Chemical Technology, Dept. of Chemistry, Aristotle University of Thessaloniki, Univ. Box 116, GR54124 Thessaloniki, Greece.

reactors, crystallizers and precipitation equipment as well as bioreactors.

Since the population balance is usually an integrodifferential equation, it can be solved only numerically for the general case. Such a numerical solution is not a trivial task and even its transformation to a set of ODE's is not a standard procedure. In the last two decades, a lot of effort has been spent for the development of numerical methods of solution of the population balance equation. These efforts have led to a variety of methods for the solution of the *spatially homogeneous* population balance with one internal variable (that is, particle volume) (see Ramkrishna (1985) and Williams and Loyalka (1991) for a review of the subject). Further development of the population balances as a simulation tool proceeds in two directions. First, the number of internal variables is increased in order to describe more realistically the population; second, population balances are combined with spatially distributed phenomena (flow, diffusion, temperature distribution) in order to achieve improved design of the corresponding equipment. The solution of the spatially distributed population balances with more than one internal variable is, of course, the ultimate goal; however, at this stage it is only feasible to concentrate either on the physical aspects of a problem, by assuming spatial homogeneity, or to tackle the geometrical complexity by keeping the physics simple (for example, a monodisperse PSD). The above two limits can be relaxed by properly adjusting the degree of approximation of the solution, with respect to internal and external coordinates. The number of studies in which spatially dependent population balances are addressed has sharply increased in the last few years. Some older typical works include combined diffusion and aerosol dynamics (Tandon and Rosner, 1996), diffusion and precipitation from the liquid phase (Wachi and Jones, 1991), and precipitation from liquid phase in turbulent flow (Senckler et al., 1995).

The phenomenon of breakage (fragmentation) is of interest in many branches of chemical engineering, from polymer degradation (Wang et al., 1995) to solids comminution (Austin, 1972), and from cell population dynamics (Mantzaris et al. 2001) to lean liquid-liquid dispersion dynamics (Ramkrishna, 1974). In all the above applications, spatially dependent effects are of paramount importance, for example, mixing of solids in comminution and convection-diffusion in the other cases. In this study, the spatial dependency is introduced in the breakage equation through a diffusion term. The resulting *breakage-diffusion population balance* has the particular advantage of linearity which permits significant analytical manipulations. Among possible fields of application of the diffusion-breakage equation is the study of polymer degradation combined with a deposition mechanism. Also, it is a first step for the study of cellular populations under nonuniform conditions in space (see Nielsen and Villadsen (1994) for cellular dynamics and Thurner et al. (2003) for cell diffusion). Another very important field of application is the interaction between breakage and spatial distribution of droplets in liquid-liquid dispersions, for example, water dispersed in oil transfer pipelines and in other flow fields (for example, Karabelas, 1977; Baker, 1988). The diffusion-breakage population balance has also been used to simulate the axial dispersion of solid particles during a continuous grinding process (Mihalyko et al., 1998). The analytical solutions derived in this work are considered useful for the

assessment of numerical methods developed for tackling of the above problems.

The structure of this work is as follows: First, the breakage-diffusion population balance is formulated and properly non-dimensionalized. Then, the general solution of the homogeneous problem (with no particle generation) is derived, based on a separation of variables procedure, which separates spatial and temporal modes. A rather extensive discussion on iterative approaches for the temporal modes follows. The Green's functions of the diffusion-breakage operator are derived, and (using their superposition) solutions of the corresponding equation are determined for an arbitrary particle generation (source) term. Next, spatial functions are given in closed form for several simple geometries. Some closed form solutions are also obtained for the temporal functions, for specific simple breakage conditions (binary random and equal-size multiple breakage). Finally, explicit results are presented and discussed from the solution of the breakage-diffusion population balance for typical conditions.

Problem Formulation

A domain A is assumed which is confined by a boundary C . In this domain particles are produced through time-dependent spatially distributed sources. The particles after their generation may undergo breakage, while they are free to diffuse from higher to lower concentration regions. The wall is assumed to be perfectly absorbing, which physically means that the particles deposit upon reaching the boundary C ; that is, there are no repulsive particle wall forces (Elimelech et al., 1995). A further assumption is that the particles are characterized only by their volume; that is, volume is the only internal variable. Thus, the population balance equation describing the evolution of particle-size distribution in time and space is of the form (Ramkrishna, 2000)

$$\frac{\partial f(x, \mathbf{r}, t)}{\partial t} = D(x) \nabla_{\mathbf{r}}^2 f(x, \mathbf{r}, t) + \int_x^\infty p(x, y) b(y) f(y, \mathbf{r}, t) dy - b(x) f(x, \mathbf{r}, t) + J(x, \mathbf{r}, t) \quad (1)$$

where t is time, \mathbf{r} is the vector of spatial coordinates, x is the particle volume, $f(x, \mathbf{r}, t)$ is the particle number density function (see Ramkrishna, 2000 for a detailed definition), $b(x)$ is the breakage rate of particle of volume x (actually, it is frequency, but the term rate is extensively used in the literature), $p(x, y)$ is the number density distribution of particles of volume x resulting from the breakup of a particle of volume y (*breakage kernel*), $D(x)$ is the diffusion coefficient of particles of volume x , and $J(x, \mathbf{r}, t)$ is the particle generation rate (source term). The breakage kernel $p(x, y)$ must satisfy the following mass conservation requirement

$$\int_0^y x p(x, y) dx = y \quad (2)$$

The number of particles resulting from breakage of a single particle of volume y is given as

$$v(y) = \int_0^y p(x, y) dx \quad (3)$$

The boundary condition of Eq. 1 is

$$f(x, \mathbf{r}, t) = 0 \text{ on } C \quad (4)$$

and the initial condition

$$f(x, \mathbf{r}, t) = f_o(x, \mathbf{r}) \text{ in } A \quad (5)$$

where f_o is the initial spatially distributed particle-size distribution.

It is more convenient to work in dimensionless variables, so the following nondimensionalization is introduced

$$x = \frac{x}{x_o}, \quad \mathbf{r} = \frac{\mathbf{r}}{L}, \quad D(x) = \frac{D(x)}{D(x_o)}, \quad b(x) = \frac{b(x)L^2}{D(x_o)},$$

$$p(x, y) = \frac{p(x, y)}{x_o}$$

$$F(x, r, t) = \frac{x_o f(x, r, t)}{N}, \quad t = \frac{D(x_o)t}{L^2},$$

$$J(x, r, t) = \frac{J(x, r, t)L^2 x_o}{D(x_o)N} \quad (6)$$

where on the lefthand side are the new dimensionless variables, and on the righthand side are the dimensional ones. The dimensionless population balance equation is

$$\frac{\partial F(x, \mathbf{r}, t)}{\partial t} = D(x) \nabla_{\mathbf{r}}^2 F(x, \mathbf{r}, t) + \int_x^\infty p(x, y) b(y) F(y, \mathbf{r}, t) dy$$

$$- b(x) F(x, \mathbf{r}, t) + J(x, \mathbf{r}, t) \quad (7)$$

The normalization variables, L for the length, x_o for the particle volume, and N for the particle-size distribution, can be arbitrarily selected. The proposed choice is a characteristic length of domain A for L , the mean particle volume and mean particle number concentration of the initial particle population (if it does exist) for x_o and N , respectively. The particular choice of time nondimensionalization (using diffusion and not breakage timescale) arises naturally since the diffusion is always present to render the balance equation consistent with the boundary conditions. However, the breakage rate may be zero, which is allowed by the particular choice of variables.

Problem Solution

Homogeneous problem ($J(x, \mathbf{r}, t) = 0$)

The source term in Eq. 7 is ignored, and it is assumed that the solution has the following separable form

$$F(x, \mathbf{r}, t) = S(\mathbf{r})T(x, t) \quad (8)$$

The well-known steps of the separation of variables procedure lead to the following two equations where λ is an arbitrary constant

$$\nabla_{\mathbf{r}}^2 S(\mathbf{r}) = -\lambda^2 S(\mathbf{r}) \quad (9)$$

$$\frac{\partial T(x, t)}{\partial t} = \int_x^\infty p(x, y) b(y) T(y, t) dy - b(x) T(x, t)$$

$$- \lambda^2 D(x) T(x, t) \quad (10)$$

From boundary condition 4, one can conclude that

$$S(\mathbf{r}) = 0 \text{ on } C \quad (11)$$

Equation 9 with boundary condition 11 is the well known Dirichlet eigenvalue problem arising in the solution of the parabolic diffusion (conduction) partial differential equation. Nontrivial solutions (eigenfunctions S_i) exist only for the eigenvalues $\lambda = \lambda_i (i=1, 2, \dots)$. This eigenvalue problem is of the Sturm-Liouville type which means that its eigenfunctions comprise an orthogonal set, that is, $\int_A S_i S_j d\mathbf{r} = 0$ for $i \neq j$. Due to the homogeneity of Eq. 9 any multiple of S_i is also an eigenfunction. For convenience, in the following, S_i will denote the orthonormal eigenfunctions; that is, normalized such that

$$\int_A S_i^2 d\mathbf{r} = 1$$

The general solution of the homogeneous equation is given by a linear superposition of the partial solutions corresponding to different eigenvalues

$$F(x, \mathbf{r}, t) = \sum_{i=1}^{\infty} T_i(x, t) S_i(\mathbf{r}) \quad (12)$$

where the functions $T_i(x, t)$ are obtained from the solution of Eq. 13

$$\frac{\partial T_i(x, t)}{\partial t} = \int_x^\infty p(x, y) b(y) T_i(y, t) dy - b(x) T_i(x, t)$$

$$- \lambda_i^2 D(x) T_i(x, t) \quad (13)$$

The initial conditions for integrating Eq 13 are determined by applying Eq. 12 for $t=0$, and using the orthonormality property of S_i , that is

$$T_i(x, 0) = \int_A F_o(x, \mathbf{r}) S_i(\mathbf{r}) d\mathbf{r} \quad (14)$$

Equation 13 is the well-known breakage equation with the addition of a linear *sink term*, which describes the evolution of

a particle-size distribution, uniform in space, undergoing breakage and deposition. Nevertheless, its general form is similar to that of the conventional breakage equation, that is

$$\frac{\partial T(x, t)}{\partial t} = \int_x^\infty A(x, y)T(y, t)dy - B(x)T(x, t) \quad (15)$$

so the same solution techniques can be used.

An important feature of the above integrodifferential equation is that (due to its linearity) the solution for any initial particle-size distribution is obtained by appropriately superposing solutions for monodisperse initial distributions. The Green's function with respect to particle size can be defined as the solution of Eq. 15 for a monodisperse initial distribution with particles of size z and is denoted as $T_\delta(x, t; z)$. The solution for an arbitrary initial PSD is of the form

$$T(x, t) = \int_0^\infty T(z, 0)T_\delta(x, t; z)dz \quad (16)$$

By substituting $T_\delta(x, 0; z) = \delta(x - z)$ in the above equation, the following identity results as a confirmation of its validity

$$T(x, 0) = \int_0^\infty T(z, 0)\delta(x - z)dz \quad (17)$$

Equation 15 can be written in its Volterra integral form and solved using the method of successive substitutions, the convergence of which has been proven by Ramkrishna (2000). It can be shown that the above method leads to a solution of the form

$$T(x, t) = T(x, 0) + \sum_{i=0}^\infty C_i(x) \frac{t^i}{i!} \quad (18)$$

At each iteration step a new term is added to the above series.

Another approach equivalent in nature, but more meaningful in physical content, has attracted researchers attention in recent years. The PSD is decomposed in generations as follows

$$T(x, t) = \sum_{i=0}^\infty T^{(g)}(x, t) \quad (19)$$

where the generation g includes all the particles which have undergone g breakage events. This approach was introduced by Liou et al. (1997) in the context of a study of microbial and cell structures for which it arises naturally. Shortly thereafter, Lensu (1998) generalized the method of generations as a mathematical tool for the study of fragmentation. He also suggested that the generation index can be an additional internal variable, and the breakage functions may be explicitly dependent on it, in addition to the size dependence.

From the mathematical point of view, the method of gener-

ations is actually the method of successive substitutions, where an iteration scheme is used differently than that leading to series (Eq. 18). Now, the key operator for the iterations is not the time derivative alone but the term

$$\frac{\partial T(x, t)}{\partial t} + B(x)T(x, t)$$

Using techniques for the integration of nonhomogeneous linear differential equations, the method of successive substitutions leads to

$$T^{(0)}(x, t) = T(x, 0)e^{-B(x)t}$$

$$T^{(g+1)}(x, t) = e^{-B(x)t} \int_x^\infty \int_0^t e^{B(x)\tau} A(x, y)T^{(g)}(y, t)dy \quad (20)$$

The first generation for the Green's function $T_\delta(x, t; z)$ can be obtained explicitly as

$$T_\delta^{(1)}(x, t; z) = e^{-B(x)t} A(x, z) \frac{1 - e^{-(B(x)-B(z))t}}{B(x) - B(z)} \quad (21)$$

By expanding the exponential term in Taylor series, the function for the first generation takes the form $e^{-B(x)t} \sum_{i=1}^\infty A_i(x, z)t^i/i!$. By substitution in the iterative scheme (Eq. 20), it can be shown (by induction) that all the generations obey the above functional form. From Eq. 19, one can deduce that the (particle size) Green's function can be written as

$$T_\delta(x, t; z) = \delta(x - z)e^{-B(z)t} + e^{-B(x)t} \sum_{i=1}^\infty C_i(x, z) \frac{t^i}{i!} \quad (22)$$

Substitution of the above series in Eq. 15, changing the summation indices and equating terms of the same power of time leads to the following recursive formula for the functions C_i ($i=1, 2, \dots, \infty$)

$$T_\delta(x, t; z) = \delta(x - z)e^{-B(z)t} + e^{-B(x)t} \sum_{i=1}^\infty C_i(x, z) \frac{t^i}{i!} \quad (22)$$

$$C_{i+1}(x, z) = \int_x^z A(x, y)C_i(y, z)dy + [B(z) - B(x)]C_i(x, z) \quad (23)$$

The above type of solution has been presented for the case of binary breakage by Ziff and McGrady (1986), and generalized for arbitrary breakage by Kostoglou and Karabelas (2001). In both cases, the expansion of the form of Eq. 22 is introduced without explanation. It is important to notice that an expansion of the type 22 is not possible for the case of an arbitrary (nonmonodisperse) initial-size distribution. This is due to the

fact that an exponential in time term (that is, as in Eq. 21) cannot survive from the integration with respect to size in Eq. 20. This restriction does not exist for $B(x)=\text{constant}$ for which a solution of the form of Eq. 22 can be found for arbitrary $T(x,0)$.

So far, three series solutions of Eq. 15 have been developed. The first (Eq. 18) is a simple power series in time, with very poor convergence properties. For a finite time, a large number of terms are needed to obtain a meaningful solution, but as time tends to infinity, the series tends to infinity as well, for a finite number of terms. The second method is an expansion not with respect to time (as the first one), but with respect to a new variable, the so-called *generation*. Each term of the expansion provides the exact size distribution of the corresponding generation for any value of time; thus, the series tends to zero as time goes to infinity for any number of terms. Of course, as the breakage time increases, more terms are needed in Eq. 19. The major disadvantage of this method is of computational nature. The series in Eq. 19 is not separable with respect to the two variables (x,t) , unlike the series in Eq. 18. This means that a 2-D recursive relation (Eq. 20) is needed to determine additional terms in the series of Eq. 19. The third method combines the advantages of the other two. The solution is separable, with a very simple form of the time terms (product of powers with an exponential Eq. 22). The recursive relation is just with respect to particle size (1-D) (Eq. 23). Furthermore, this method has the nice convergence properties of the second method. As time goes to infinity, the series tends to zero for any number of terms due to the exponential. This method can be directly used only for a monodisperse initial distribution, but the superposition property enables its application for arbitrary $T(x,0)$. For the particular case $B(x)=\text{constant}$, the iterative scheme of Eq. 23 is simplified considerably. In this case, the second and third iterative solution methods coincide, and the term i of the series 22 corresponds to the i th generation of the particle population.

If the fragment-size distribution resulting from a single breakage event depends only on the relative size between the fragments and parent particle sizes, and is independent of the absolute size of the parent particle, then the breakage kernel is called homogeneous and can be written in the form $p(x,y)=\varphi(x,y)/y$. The breakage rate is homogeneous only if it is of a power law form; that is, $b(x)\propto x^b$.

For homogeneous breakage kernel and rate, the function $(1/z)T_\delta((x/z), B(z)t)$ is invariant with respect to the initial particle size z . This means that one can solve Eq. 15 for the particle size Green's function, with a particular value of z (usually the value $z=1$ is preferred), and then determine all the particle size Green's functions for arbitrary value of z by using the above invariance (changing the scaling of the particle size, time, and PSD). This is a very important property since Eq. 15 need only be solved just for one monodisperse initial distribution in order to determine the size distribution evolution for an arbitrary initial distribution, using the superposition principle.

Generalized Green's functions for the diffusion-breakage equation

The Green's functions are of special interest for the study of the linear equations of mathematical physics (Courant and Hilbert, 1989) and transport phenomena (Carslaw and Jaeger, 1959). Their major significance is that they can be used to construct solutions of a nonhomogeneous problem with arbitrary sources and bound-

ary conditions, based on the solution of the corresponding homogeneous problem. The generalized Green's function for the problem studied here represents the particle-size distribution evolving in time and space for an instantaneous point source of monodisperse particles of size z , located at \mathbf{r}_0 and activated at time τ . The Green's function $G(x, \mathbf{r}, t; z, \mathbf{r}_0, \tau)$ can be obtained from the solution of the following equation

$$\frac{\partial G}{\partial t} = D(x)\nabla_r^2 G + \int_x^\infty p(x, y)b(y)Gdy - b(x)G + \delta(x-z)\delta(\mathbf{r}-\mathbf{r}_0)\delta(t-\tau) \quad (24)$$

with initial condition

$$G = 0 \text{ on } C$$

The solution of this equation is

$$G(x, \mathbf{r}, t; z, \mathbf{r}_0, \tau) = \sum_{i=1}^{\infty} T_{i\delta}(x, t-\tau; z)S_i(\mathbf{r}_0)S_i(\mathbf{r})U(t-\tau) \quad (25)$$

where $U(t)$ is the Heavyside function (equal to 1 for $t \geq 0$ and 0 for $t < 0$). The validity of this solution can be checked by substitution in Eq. 24. For $t \neq \tau$ the homogeneous terms are zero as the series 25 has the general form of the solution of the homogeneous Eq. 12. At $t=\tau$ the time differentiation of the Heavyside function leads to the Dirac delta function with respect to time. Also, using the orthonormal properties of the space functions, the Dirac delta function with respect to space can be written as

$$\delta(\mathbf{r}-\mathbf{r}_0) = \sum_{i=1}^{\infty} S_i(\mathbf{r}_0)S_i(\mathbf{r}) \quad (26)$$

Finally, the size Green's function $T_{i\delta}$ is related to the Dirac delta function with respect to particle size since by definition $T_{i\delta}(x, 0; z) = \delta(x-z)$.

Solution for a general source term

Equation 7 with an arbitrary source term can be decomposed in a series of equations with simpler source terms. If the initial source term can be written as a weighted sum of simpler terms, then the solution of the initial equation is the same weighted sum of solutions of the simpler equation as a consequence of linearity. The arbitrary source term is chosen to be decomposed in products of Dirac delta functions, which means that the corresponding solutions are the Green's functions. The source function is written as

$$J(x, \mathbf{r}, t) = \int_0^\infty \int_A \int_0^t J(z, \mathbf{r}_0, \tau) \delta(x-z) \delta(\mathbf{r}-\mathbf{r}_0) \delta(t-\tau) d\tau d\mathbf{r}_0 dz \quad (27)$$

Using the corresponding superposition of Green's functions, the solution for the general source term $J(x, \mathbf{r}, t)$ can be constructed as

$$F(x, \mathbf{r}, t) = \int_0^\infty \int_{\mathbf{A}} \int_0^t J(z, \mathbf{r}_o, \tau) G(x, \mathbf{r}, t; z, \mathbf{r}_o, \tau) d\tau d\mathbf{r}_o dz \quad (28)$$

This solution is for the case of no particles at $t=0$. To account for an initial particle-size distribution $F_o(x, \mathbf{r})$, the term $F_o(x, \mathbf{r})\delta(x - z)\delta(\mathbf{r} - \mathbf{r}_o)\delta(t)$ must be added to the source term of Eq. 7. The general solution of the expanded Eq. 7 is given in closed form as

$$F(x, \mathbf{r}, t) = \int_0^\infty \int_{\mathbf{A}} \int_0^t J(z, \mathbf{r}_o, \tau) G(x, \mathbf{r}, t; z, \mathbf{r}_o, \tau) d\tau d\mathbf{r}_o dz + \int_0^\infty \int_{\mathbf{A}} F_o(z, \mathbf{r}_o) G(x, \mathbf{r}, t; z, \mathbf{r}_o, 0) d\mathbf{r}_o dz \quad (29a)$$

$$G(x, \mathbf{r}, t; z, \mathbf{r}_o, \tau) = \sum_{i=1}^\infty T_{i\delta}(x, t - \tau; z) S_i(\mathbf{r}_o) S_i(\mathbf{r}) U(t - \tau) \quad (29b)$$

$$T_{i\delta}(x, t; z) = \delta(x - z) e^{-[b(z) + \lambda_i^2 D(z)]t} + e^{-[b(z) + \lambda_i^2 D(z)]t} \sum_{k=1}^\infty C_{i,k}(x, z) \frac{t^k}{k!} \quad (29c)$$

$$C_{i,k+1}(x, z) = \int_x^z p(x, y) b(y) C_{i,k}(y, z) dy + [b(z) + \lambda_i^2 D(z) - b(x) - \lambda_i^2 D(x)] C_{i,k}(x, z) \quad (29d)$$

$$C_{i,1} = (x, z) = p(x, z) b(z) \quad (29e)$$

Some special cases

Space functions S_i . For the general case of a domain \mathbf{A} of arbitrary shape, the eigenvalue problem 9, can only be solved numerically; however, analytical solutions exist for some simple shapes of \mathbf{A} . These solutions will be given for the 3-D case only, since solutions for two and one dimensions can be easily deduced from the 3-D ones. The shapes of \mathbf{A} for which solution to the eigenvalue problem 9 exists are the orthogonal parallelepiped, the cylinder and the sphere.

(a) orthogonal parallelepiped

A Cartesian coordinate system (z_1, z_2, z_3) is used with dimensions of parallelepiped L_1, L_2, L_3 .

The eigenvalues are

$$\lambda_i = \left(\frac{k^2}{L_1^2} + \frac{m^2}{L_2^2} + \frac{n^2}{L_3^2} \right)^{1/2} \pi \quad (30)$$

$k, m, n = 1, 2, 3, 4, \dots$

with the corresponding eigenfunctions

$$S_i = \left(\sqrt{\frac{2}{L_1}} \sin\left(\frac{k\pi}{L_1} z_1\right) \right) \left(\sqrt{\frac{2}{L_2}} \sin\left(\frac{m\pi}{L_2} z_2\right) \right) \left(\sqrt{\frac{2}{L_3}} \sin\left(\frac{n\pi}{L_3} z_3\right) \right) \quad (31)$$

A differently ordered triad (k, m, n) corresponds to each value of index i . If some dimensions are to be disregarded, the corresponding terms in Eqs. 30 and 31 are omitted.

(b) cylinder

A cylindrical coordinate system (r, φ, z_1) is employed, where the radius of the cylinder is R and its length L_1 .

The eigenvalues are

$$\lambda_i = (\beta_{m,n}^2 + k^2)^{1/2} \quad (32)$$

where $k, m=1, 2, 3, \dots, n=0, 1, 2, \dots$ and $\beta_{m,n}$ is the m th solution of the algebraic equation $(J_n(\beta R)=0)$. Here J_n is the Bessel function of first kind and order n .

The corresponding eigenfunctions are

$$S_i(r, z_1, \varphi) = \left(\frac{\sqrt{2}}{R} \frac{J_n(\beta_m r)}{J'_n(\beta_m R)} \right) \times \left(\sqrt{\frac{2}{L_1}} \sin\left(\frac{k\pi}{L_1} z_1\right) \right) \left(\frac{\pi^{-1/2} \sin(n\varphi)}{\pi^{-1/2} \cos(n\varphi)} \right) \quad (33)$$

where distinct eigenfunctions with different index i exist for the two different ϕ functions. For $n=0$, $(2\pi)^{-1/2}$ must substitute $\pi^{-1/2}$.

For an axisymmetric problem (for example, a ring source) only the eigenvalues and eigenfunctions with $n=0$ must be retained. For the infinite cylinder problem with a line source, k is set equal to zero in eigenvalue relation Eq. 32, and the z term in Eq. 33 is neglected.

(c) sphere

In a spherical coordinate system (r, θ, ϕ) , R is the radius of the spherical domain \mathbf{A} .

The eigenvalues are

$$\lambda_i = \beta_{k,n} \quad (34)$$

where

$$k = 1, 2, 3, \dots, m = 0, 1, 2, \dots, n = 0, 1, 2, \dots$$

and $\beta_{k,n}$ is the k th root of the Bessel function of order $n+1/2$; i. e

$$J_{n+1/2}(\beta_{k,n}) = 0.$$

The corresponding eigenfunctions are

$$S_i(r, \theta, \varphi) = \left(\frac{\sqrt{2}}{R} \frac{(\lambda_k r)^{-1/2} J_{n+1/2}(\beta_{k,n} r)}{J'_{n+1/2}(\beta_{k,n} R)} \right) \times \left(\sqrt{\frac{2(n+1)(n-m)!}{2(n+m)!}} P_n^m(\cos \theta) \right) \left(\frac{\pi^{-1/2} \sin(m\varphi)}{\pi^{-1/2} \cos(m\varphi)} \right) \quad (35)$$

where P_n^m are the associated Legendre polynomials. For $m = 0$, $(2\pi)^{-1/2}$ must substitute $\pi^{-1/2}$. For the case of axial symmetry m must be set equal to zero in Eqs 34 and 35.

Time functions $T_{i\delta}$. Closed form solutions for the functions $T_{i\delta}$ can be obtained for some simple (yet extensively employed in practical applications) forms of the functions $D(x)$, $b(x)$, $p(x,y)$. A power law dependence on the particle volume is assumed for the diffusivity $D(x)$, and for the breakage rate $b(x)$. This is fully accepted for the diffusivity and widely used for the breakage rate in the literature. In dimensionless form it can be written as $b(x) = \alpha_1 x^b$, $D(x) = \alpha_2 x^d$. Although, for the particular nondimensionalization used here (Eq. 6) α_2 is by definition equal to 1, it is retained in the following analysis to accommodate a different nondimensionalization. Results will be presented for the case of random binary breakage where $p(x,y) = 2/y$, and equal-sized breakage in v fragments where $p(x,y) = v/y \delta(x - y/v)$. For the case of binary breakage, the uniform and equal size breakage kernels are the two limits ($m=0$ and $m=\infty$, respectively) of the general breakage kernel $p(x,y) = C(x/y)^m (1 - (x/y))^m$ where C is the normalization constant. This kernel and especially its two limits have been extensively used for the simulation of molecular cracking (McCoy and Wang, 1994), polymer degradation (Wang et al., 1995), and cell population dynamics (Mantzaris et al., 2001). A very interesting generalization of the homogeneous fragmentation kernel can be found in the recent work of Diemer and Olson (2002b).

(a) binary random breakage with $b=d$

This case in which the diffusivity and the breakage rate have the same particle size dependence is not very realistic since in practice $b > 0$ and $d < 0$. Nevertheless, it admits an explicit solution for the function. The equation that must be solved is

$$\frac{\partial T_{i\delta}(x, t; z)}{\partial t} = 2\alpha_1 \int_x^\infty y^{d-1} T_{i\delta}(y, t; z) dy - (\alpha_1 + \alpha_2 \lambda_i^2) x^d T_{i\delta}(x, t; z) \quad (36)$$

with

$$T_{i\delta}(x, 0; z) = \delta(x - z)$$

According to the analysis in the previous section, the solution of the above equation is

$$T_{i\delta}(x, t; z) = \delta(x - z) e^{-(\alpha_1 + \alpha_2 \lambda_i^2) z^d t} + e^{-(\alpha_1 + \alpha_2 \lambda_i^2) z^d t} \sum_{k=1}^{\infty} C_k(x, z) \frac{t^k}{k!} \quad (37)$$

where

$$C_{k+1}(x, z) = 2\alpha_1 \int_x^z y^{d-1} C_k(y, z) dy + (\alpha_1 + \alpha_2 \lambda_i^2) (z^d - x^d) C_k(x, z) \quad (37a)$$

$$C_1 = 2\alpha_1 z^{b-1} \quad (37b)$$

In order to find a closed form relation for the functions $C_k(x, z)$, it is assumed that

$$C_k(x, z) = E_k(z^d - x^d)^{k-1} \quad (38)$$

Substituting in the recursive formula 37a, and performing the integration leads to the following recursive relation for E_k 's

$$E_{k+1} = \left(\frac{2\alpha_1}{dk} + \alpha_1 + \lambda_i^2 \alpha_2 \right) E_k \quad (39)$$

or in explicit form

$$E_k = 2\alpha_1 z^{d-1} \prod_{j=1}^{k-1} \left(\frac{2\alpha_1}{dj} + \alpha_1 + \lambda_i^2 \alpha_2 \right) \quad (40)$$

(b) equal size breakage in v fragments

In this particular case the method of generations is simpler than the iterative scheme due to the fact that the functional form of the generations is known at the outset (Dirac functions) and only time-dependent coefficients must be determined. In general, it can be written as

$$T_{i\delta}(x, t; z) = \sum_{k=0}^{\infty} f_k(t) \delta(x - v^{-k} z) \quad (41)$$

where the time functions f_k result from the solution of the following system of ODE's

$$\frac{df_k}{dt} = v\alpha_1 (zv^{-k+1})^b f_{k-1} - [\alpha_1 (zv^{-k})^b + \alpha_2 \lambda_i^2 (zv^{-k})^d] f_k \quad (42)$$

where

$$f_0 = \delta(x - z) e^{-(\alpha_1 z^b + \alpha_2 \lambda_i^2 z^d) t}$$

and

$$f_k(0) = 0$$

From the type of system 42, it is inferred that the functions f_k have the following form

$$f_k = \sum_{j=1}^k c_{k,j} e^{-[\alpha_1 (zv^{-j})^b + \alpha_2 \lambda_i^2 (zv^{-j})^d] t} \quad (43)$$

Substituting into 42 and after some algebra leads to the following relations for the unknown coefficients $c_{k,j}$ ($k=0,1,2, \dots, j=0,1,2, \dots, k$)

$$c_{k,j} = \frac{v\alpha_1(zv^{-k+1})^b}{[\alpha_1(zv^{-k})^b + \alpha_2\lambda_i^2(zv^{-k})^d] - [\alpha_1(zv^{-j})^b + \alpha_2\lambda_i^2(zv^{-j})^d]} c_{k-1,j} \quad (44)$$

The initial condition $f_k(0) = 0$ implies that $c_{k,k} = - \sum_{j=0}^{k-1} c_{k,j}$ (45)

Equations 44 and 45 can be used sequentially to compute $c_{k,j}$ starting from $c_{0,0}=1$.

(c) binary random breakage ($b \neq d$)

This case is a realistic one and although an explicit solution is not possible, the iterative scheme 29d can be transformed into systems of ODE's, which can be solved with arbitrary prespecified accuracy using an ODE integrator. For each value of i (each eigenvalue), the following system of ODE's must be solved for the functions $C_{i,k}(x,z)$ ($k=1,2,3, \dots$)

$$\begin{aligned} \frac{dC_{i,k+1}(x,z)}{dx} = & -2\alpha_1 x^{b-1} C_{i,k}(x,z) \\ & - [\alpha_1 b x^{b-1} - \lambda_i^2 \alpha_2 d x^{d-1}] C_{i,k}(x,z) \\ & + [\alpha_1 z^b + \lambda_i^2 \alpha_2 z^d - \alpha_1 x^b + \lambda_i^2 \alpha_2 x^d] \frac{dC_{i,k}(x,z)}{dx} \end{aligned} \quad (46)$$

where

$$C_{i,1}(x,z) = 2\alpha_1 z^{b-1} \quad (47)$$

The initial conditions for the above system are $C_{i,k+1}(0)=0$.

Results and Discussion

The main goal of this work is the solution of the transient diffusion-breakage equation via a decomposition into time and space components. Depending on the breakage functions and the problem geometry, the corresponding subproblems can be solved either analytically or numerically. Analytical solutions of the spatial problem have been presented earlier for some simple geometries. For an arbitrary geometry, Eq. 9 can be discretized using finite difference or finite element methods, and transformed into an algebraic eigenvalue problem which can be solved by employing appropriate algorithms. This procedure is not very efficient since the space functions S_i are strongly oscillating with a frequency increasing with index i ; thus, a large number of discretization points are required for their representation. The real strength of the decomposition method manifests itself in cases where the space functions are given in closed form. As regards to the time functions, they can be determined by solving equations very similar to the conventional fragmentation equation; thus, the whole toolbox of methods for solving the fragmentation problem can be employed. This toolbox contains various types of sectional methods (Kumar and Ramkrishna, 1996; Vanni, 1999), moment methods (Kostoglou and Karabelas, 2002; Madras and McCoy,

1998; Diemer and Olson, 2002a), and even Monte Carlo approaches (Mishra, 2000; Lee and Matsoukas, 2000), which are of special significance for the case of more than one internal variable in the population balance. Even if numerical solution is required for the time functions, it is advantageous to solve the decomposed problem than the original one (provided that closed form solution for the space function exists). In the following, it will be shown how the above analysis can be used to extract explicit results for some simple cases.

Uniform initial concentration of monodisperse particles undergoing equal-size fragmentation

The number concentration of particles is N and their size x_0 ; that is, these variables are used for the normalization. The solution of this problem is

$$\begin{aligned} F(x, \mathbf{r}, t) = & \int_A G(x, \mathbf{r}, t; 1, \mathbf{r}_o, 0) d\mathbf{r}_o \\ = & \sum_{k=1}^{\infty} T_{k\delta}(x, t; 1) S_i(\mathbf{r}) \int_A S_i(\mathbf{r}_o) d\mathbf{r}_o \end{aligned} \quad (48)$$

For the particular case in which diffusion takes place in a slab, with two dimensions infinite and only the third finite, the geometry is 1-D cartesian. Using Eqs. 41–44 for the time functions, and Eqs. 30 and 31 for the space ones, the following result is obtained

$$\begin{aligned} F(x, z_1, t) = & \sum_{k=0}^{\infty} \sum_{i=1,3,5,\dots}^k \delta(x \\ & - v^{-k}) c_{k,j}^{(i)} e^{-(\alpha_1 v^{-jb} + \lambda_i^2 v^{-jd})t} \frac{4}{i\pi} \sin(i\pi z_1) \end{aligned} \quad (49)$$

where the coefficients $c_{k,j}^{(i)}$ can be found using the following set of relations

$$c_{k,j}^{(i)} = \frac{\alpha_1 v^{-(k+1)b+1}}{(\alpha_1 v^{-kb} + \lambda_i^2 v^{-kd}) - (\alpha_1 v^{-jb} + \lambda_i^2 v^{-jd})} \quad (50)$$

$$c_{0,0}^{(i)} = 1 \quad (50a)$$

$$c_{k,k}^{(i)} = - \sum_{j=0}^{k-1} c_{k,j}^{(i)} \quad (50b)$$

The flux of particle at the boundary $z_1=0$ of this domain (that is, the deposition rate) is given as

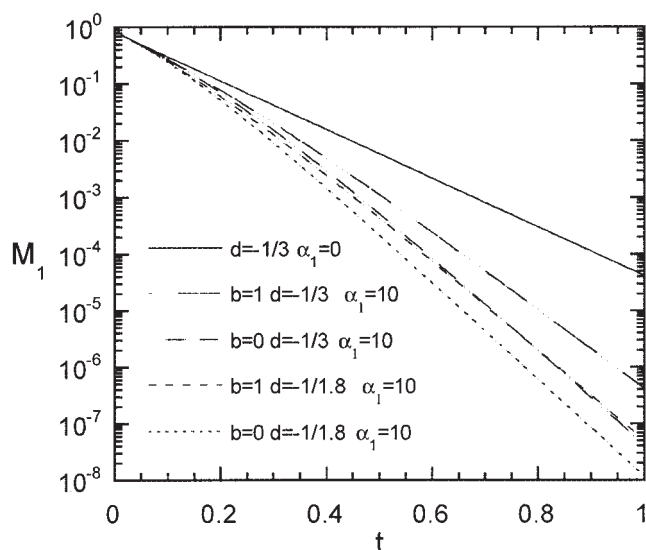


Figure 1. Evolution of the dimensionless total mass of particles existing in a slab (undergoing diffusion and binary equal size fragmentation) for several values of the problem parameters.

$$Q(x, t) = -D(x) \left(\frac{\partial F(x, z_1, t)}{\partial z_1} \right)_{z_1=0} = 4 \sum_{k=0}^{\infty} \sum_{i=1,3,5,\dots} \sum_{j=0}^k v^{-kd} \delta(x - v^{-k}) c_{k,j}^{(i)} e^{-(\alpha_1 v^{-jb} + \lambda_1^2 v^{-jd})t} \quad (51)$$

The general m-moment of particles remaining in the domain A is of special interest and it can be computed from

$$M_m(t) = \int_0^1 \int_0^{\infty} x^m F(x, z_1, t) dx dz_1 = \sum_{k=0}^{\infty} \sum_{i=1,3,5,\dots} \sum_{j=0}^k v^{-km} c_{k,j}^{(i)} e^{-(\alpha_1 v^{-jb} + \lambda_1^2 v^{-jd})t} \frac{8}{(i\pi)^2} \quad (52)$$

The evolution of the total mass and number of particles remaining in the domain under consideration is plotted in Figures 1 and 2, for typical values of the problem parameters. The values used for the breakage rate exponent are $b=0$ (size independent breakage) and $b=1$ (size-dependent breakage); for the diffusion coefficient $d=-1/3$ (spherical particles), and $d=-1/1.8$ (diffusion limited aggregates). The case of no breakage is shown for reference. It is obvious from Figure 1 that fragmentation is very efficient in enhancing indirectly the deposition rate, and consequently in reducing the total particle mass in the system, because of the higher diffusivity of the small particles produced by breakage. The reduction of the total particle mass is faster as the breakage rate exponent decreases from one to zero, because in the first case breakage slows down as the particles become smaller, but in the second case the particle size decreases continuously (and the diffusivity increases correspondingly). The total particle mass decreases faster as the exponent of the diffusion coefficient decreases (becoming more negative). If this exponent was

positive, the breakage would have a negative effect on the deposition rate.

The corresponding evolution of the total particle number is shown in Figure 2. At small times, particle breakage dominates over diffusion, and the total particle number is larger than that of the no-breakage case. After some time, the reduction of the particle size leads to enhanced diffusion which dominates compared to breakage, so the total particle number decreases with respect to the no-breakage case. The influence of the breakage rate and of the diffusivity exponents on the evolution of total particle number is similar to that for the total particle mass.

The evolution of the number flux of particles at $x=0$ (deposition rate) is shown in Figure 3 for the case $b=1$, $d=-1/3$, $\alpha_1=10$. At small times, the flux of primary particles has a singularity and is proportional to $t^{-1/2}$ as in the case of no breakage. At large times, this flux decreases faster than the no-breakage case. The flux of the fragments initially increases and then decreases after passing through a maximum. The latter occurs at longer times and has a smaller value as the generation index increases. Figure 4 is similar to Figure 3 but for $b=0$, $d=-1/1.8$, $\alpha_1=10$. In this case, the extent of breakage is larger, so the flux is significant for more generations of particles. The local number concentration for particles of several generations is shown in Figure 5 for the case $b=0$, $d=-1/1.8$, $\alpha_1=10$ at time $t=0.1$. The concentration profiles are bell-shaped for all generations. The extent of breakage is sufficient to lead to greater concentration of second and first generation particles compared to parent (primary) particles throughout the domain.

A continuous point source of monodisperse particles undergoing equal-size fragmentation

The source location is at \mathbf{r}_0 , and its strength is equal to S particles/s. The appropriate normalization variables are the size of the monodisperse particles for x_0 and $N=SL^2/D(X_0)$

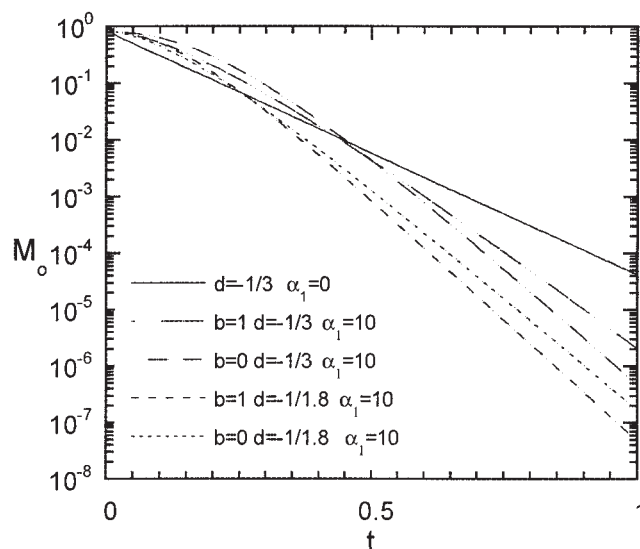


Figure 2. Evolution of the dimensionless total number of particles existing in a slab (undergoing diffusion and binary equal size fragmentation) for several values of the problem parameters.

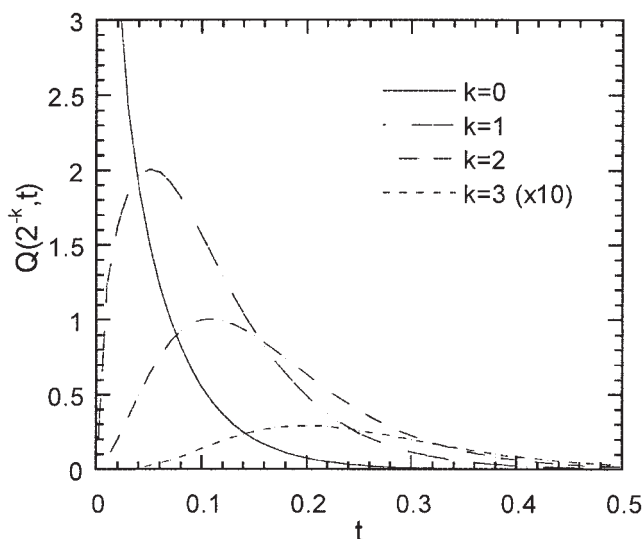


Figure 3. Dimensionless number flux of particles from the edge of the slab for binary equal size breakage with $b=1, d=-1/3, \alpha_1=10$.

Results are shown for parent particles and the first three generations.

$$F(x, \mathbf{r}, t) = \int_0^t G(x, \mathbf{r}, t; 1, \mathbf{r}_o, \tau) d\tau$$

$$= \sum_{i=1}^{\infty} \int_0^t T_{i\delta}(x, t - \tau, 1) d\tau S_i(\mathbf{r}) S_i(\mathbf{r}_o) \quad (53)$$

For the case of 1-D diffusion in a slab and equal size fragmentation, integration with respect to time can be performed analytically leading to

$$F(x, z_1, t) = \sum_{k=0}^{\infty} \sum_{i=1}^{\infty} \sum_{j=0}^k \delta(x - v^{-k}) \cdot c_{k,j}^{(i)} \frac{1 - e^{-(\alpha_1 v^{-jb} + \lambda_i^2 v^{-jd})t}}{\alpha_1 v^{-jb} + \lambda_i^2 v^{-jd}} 2 \sin(i\pi z_1) \sin(i\pi z_{1o}) \quad (54)$$

where the coefficients $c_{k,j}^{(i)}$ are given by Eq. 50. The deposition rate $Q(x, t)$ in this case is given as

$$Q(x, t) = 2\pi \sum_{k=0}^{\infty} \sum_{i=1}^{\infty} \sum_{j=0}^k v^{-kd} \delta(x - v^{-k}) \cdot c_{k,j}^{(i)} \frac{1 - e^{-(\alpha_1 v^{-jb} + \lambda_i^2 v^{-jd})t}}{(\alpha_1 v^{-jb} + \lambda_i^2 v^{-jd})} i(-1)^{i+1} \sin(i\pi z_{1o}) \quad (55)$$

Some results are shown here for the case of a source located at $z_{1o}=1/2$ and $b=1/2, d=-1/3, \alpha_1=10$.

The evolution of the number flux of particles at the boundary $z_1=0$ of the domain for particles of several generations is shown in Figure 6. The flux of the primary particles is different than that without breakage, even in the limit of small times since, at the moment particles reach the boundary by diffusion, they have already undergone considerable breakage. Another difference compared to the previously studied case is that the fluxes, after an initial period of increase, reach a steady state. The latter corresponds to the steady-state solution of the situation, whereby the rate of particles produced at the source is equal to that of particles disappearing by deposition. The steady-state solution can be obtained by setting $t=\infty$ (eliminating the exponential term) in Eq. 54.

The steady-state number concentration distribution for particles of several generations is shown in Figure 7. The spatial distribution of the initial particles is sharper than that of fragments due to the existence of the source. Although close to the source the number of primary particles is greater than that of other generations, the situation is different far from the source where the second generation prevails. The shape of the spatial distribution of the generations is similar to those of the previous case (uniform initial concentration). The evolution of the spatial-concentration distribution of primary and first generation particles from zero to the steady-state, can be deduced from Figure 8; the higher the generation index the slower the attainment of the steady state.

Using Eq. 53, the evolution of the particle-size distribution can be obtained for higher spatial dimensions. For example, if the domain \mathbf{A} has the shape of a rectangle with side length L , and the point source is located at the dimensionless coordinates z_{1o}, z_{2o} , the PSD is given as

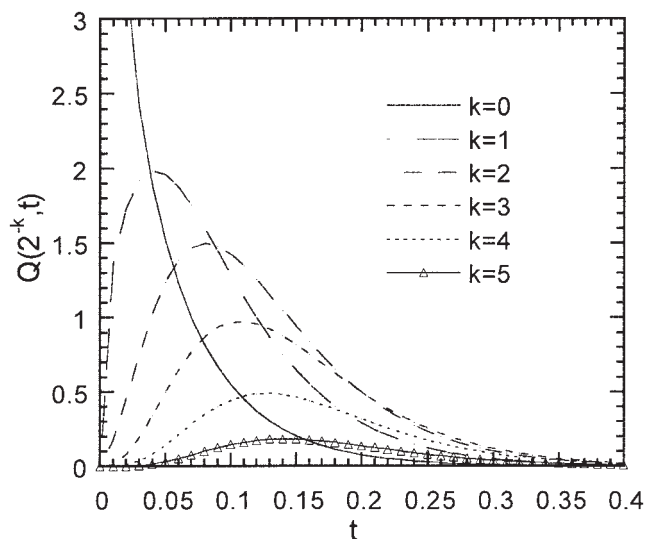


Figure 4. Dimensionless number flux of particles from the edge of the slab for binary equal size breakage with $b=0, d=-1/1.8, \alpha_1=10$.

Results are shown for parent particles and the first five generations.

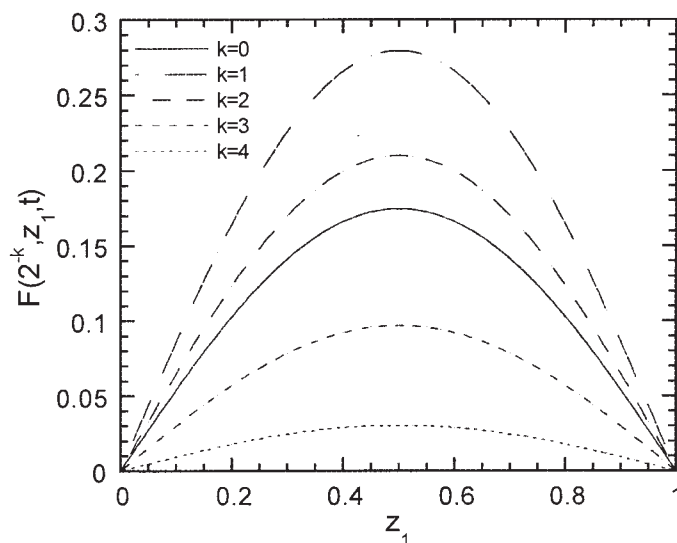


Figure 5. Spatial concentration distribution of particles along the slab for binary equal size breakage and $b=0, d=-1/1.8, \alpha_1=10$ at $t=0.1$.

Results are shown for parent particles and the first four generations.

$$F(x, z_1, z_2, t) = \sum_{k=0}^{\infty} \sum_{i_1=1}^{\infty} \sum_{i_2=1}^{\infty} \sum_{j=0}^k \delta(x - v^{-k}) \cdot c_{k,j}^{(i_1, i_2)} \frac{1 - e^{-(\alpha_1 v^{-jb} + \lambda^2(i_1, i_2) v^{-jd})t}}{(\alpha_1 v^{-jb} + \lambda^2(i_1, i_2) v^{-jd})} \times 4 \sin(i_1 \pi z_{1o}) \sin(i_2 \pi z_{2o}) \sin(i_1 \pi z_1) \sin(i_2 \pi z_2) \quad (56)$$

The coefficients $c_{k,j}^{(i_1, i_2)}$ can be determined by recursive relations similar to those for coefficients $c_{k,j}^{(i)}$, but with $\lambda(i_1, i_2) = (i_1^2 + i_2^2)^{0.5} \pi$ instead of λ_i .

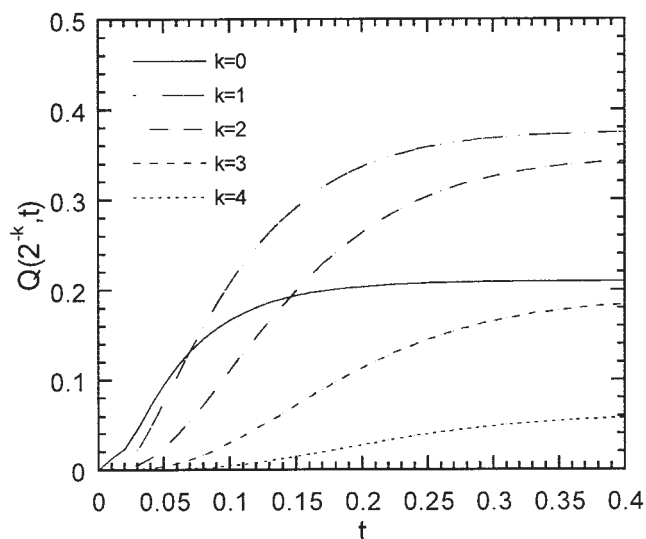


Figure 6. Dimensionless number flux of particles from the edge of the slab for binary equal size breakage with $b=1/2, d=-1/3, \alpha_1=10$, and a continuous point source at $z_1=1/2$.

Results are shown for parent particles and the first four generations.

Figure 9 shows the concentration contours of the primary particles and the first three generations at steady state, for the case of a continuous point source at the point $(1/4, 1/3)$ in a rectangular domain; other parameters are $d=-1/3, b=1, \alpha_1=10$. Under these particular conditions, as the generation index increases, the location of the maximum concentration moves toward the center of the rectangle and the contour plot tends to be more symmetric. This behavior is related to the fact that the number of fragments tends to increase as the residence time in the domain **A** increases. This residence time is proportional to the distance from the source.

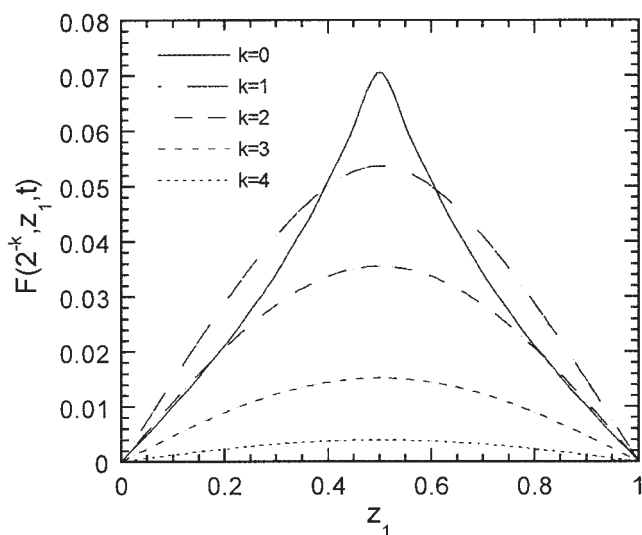


Figure 7. Steady-state spatial concentration distribution of particles along the slab for binary equal size breakage with $b=1/2, d=-1/3, \alpha_1=10$, and a continuous point source at $z_1=0.5$.

Results are shown for parent particles and the first four generations.

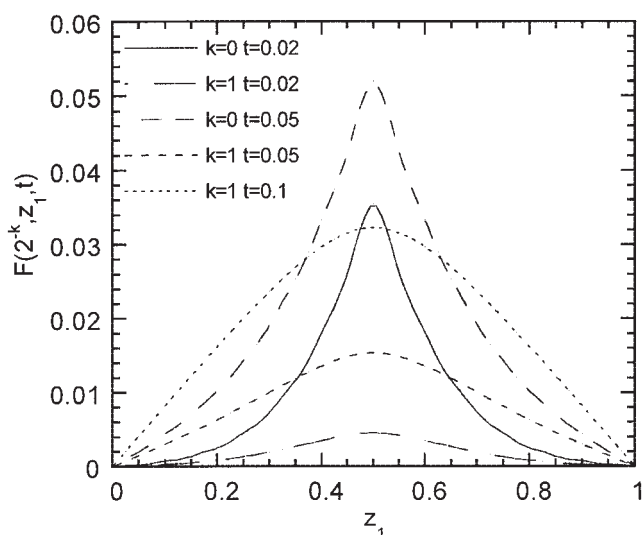


Figure 8. Transient spatial-concentration distribution of particles along the slab for binary equal size breakage with $b=1/2, d=-1/3$, $\alpha_1=10$, and a continuous point source at $z_1=1/2$.

Results are shown for parent particles and the first generation at several time values.

However, deposition tends to reduce particle concentration close to the boundary. It follows that the locus of maximum concentration for fragments of higher generation must be as far

as possible, both from the source and the boundary, that is, at the center of the rectangle.

A continuous point source of monodisperse particles undergoing random binary fragmentation

The general solution for this case is represented by Eq. 53, where the functions are given in Eq. 37, and the functions can be computed from the solution of the system of ODE's (Eq. 46). The normalization used in this case is the same as that of the previous case. Thus, the particle distribution can be determined in a compact form by

$$F(x, \mathbf{r}, t) = \sum_{i=1}^{\infty} \left[\delta(x-1) \frac{1 - e^{-(\alpha_1 + \lambda_i^2)t}}{\alpha_1 + \lambda_i^2} + \sum_{k=1}^{\infty} C_{i,k}(x) \left(\sum_{j=0}^k \frac{t^j e^{-(\alpha_1 + \lambda_i^2)t}}{(\alpha_1 + \lambda_i^2)^{k-j+1} (k-j)!} - \frac{1}{(\alpha_1 + \lambda_i^2)^{k+1} k!} \right) \right] S_i(\mathbf{r}) S_i(\mathbf{r}_0) \quad (57)$$

where the functions $C_{i,k}$ are obtained by solving the following system of ODE's ($k=2,3,4, \dots$)

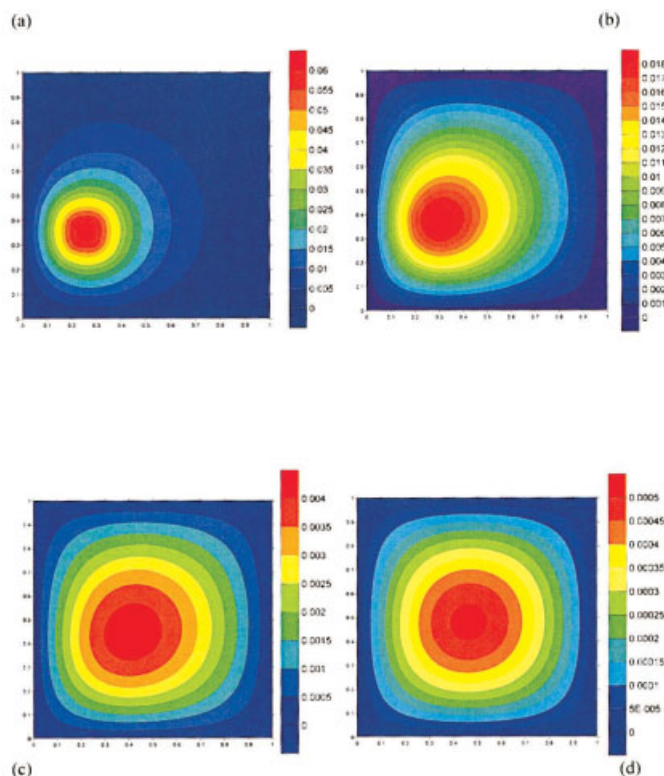


Figure 9. Steady-state spatial concentration distribution of particles in a rectangular domain for binary equal size breakage with $b=1/2, d=-1/3$, $\alpha_1=10$, and a continuous point source at $z_1=1/4, z_2=1/3$.

Results are shown for parent particles (a) and the first three generations (b),(c),(d), respectively.

$$\frac{dC_{i,k+l}(x)}{dx} = -2\alpha_i x^{b-1} C_{i,k}(x) - [\alpha_i b x^{b-1} + \lambda_i^2 x^{d-1}] C_{i,k}(x) + [\alpha_i + \lambda_i^2 - \alpha_i x^b - \lambda_i^2 x^d] \frac{dC_{i,k}(x)}{dx} \quad (58)$$

with $C_{i,1}=2\alpha_i$ and $C_{i,k}(1)=0$.

In case of no breakage $\alpha_i=0$, and all the functions $C_{i,k}$ are zero, Eq. 57 degenerates to the solution of diffusion equation for monodisperse particles. If the terms corresponding to diffusion (those which include λ_i) are omitted then the remaining equation represents pure breakage and can be solved in closed form (Ziff and McGrady, 1986). Finally, a closed-form solution has already been given for $b=d$ (Eq. 38). In any other case the above system has to be solved numerically. In this work, an explicit Runge-Kutta integrator with self-adjustable step and specified accuracy is used for this purpose (Press et al. 1992).

It is interesting to next analyze the case of size-dependent breakage with $b=1$. If additionally $d=1$, the function $C_{i,k}(x)$ is proportional to $(1-x)^{k-1}$ (see Eq. 38 for $b=d=1$). For $d=0$ the functions $C_{i,k}(x)$ do not depend on i since the terms with i in Eq. 58 are eliminated. It can be shown that in this case $C_{i,k}(x)$ are also proportional to $(1-x)^{k-1}$. Between the above cases, the functions $C_{i,k}(x)$ are positive decreasing functions of x . The value $C_{i,k}(0)$ increases with k , but the series in Eq. 57 converges fast due to the factorial $k!$ in the denominator. The situation changes when the exponent d takes negative values. In this case, the functions $C_{i,k}(x)$ diverge as x goes to zero; they can also take negative values. Although in principle, the series (Eq. 37) converges, the number of terms required for small values of x is very large, making the use of the method difficult. Furthermore, as the mode index i increases, the corresponding functions tend to diverge faster making convergence even more difficult. This is anticipated by the fast elimination with time of the higher order modes.

In Figure 10, the functions $C_{i,k}$ for $b=1$, $d<-1/3$ and are plotted ($i=1$ and k between 2 and 5). All these functions

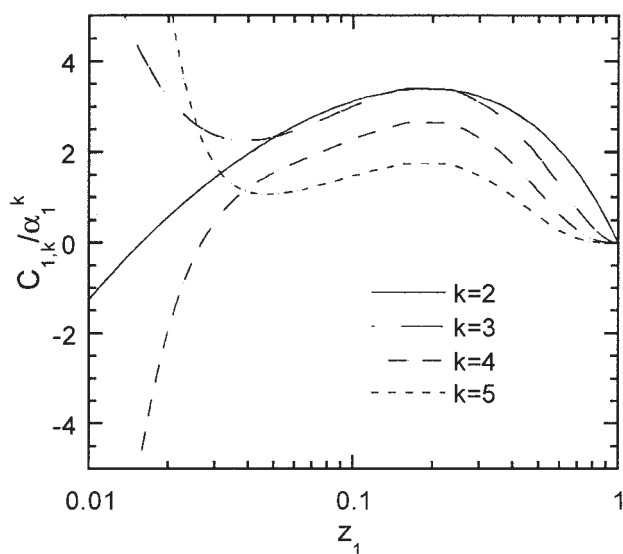


Figure 10. Functions $C_{1,k}$ (see Eq. 58) for $k=2$ to 5 and $b=1$, $d=-1/3$, $\alpha_1=10$.

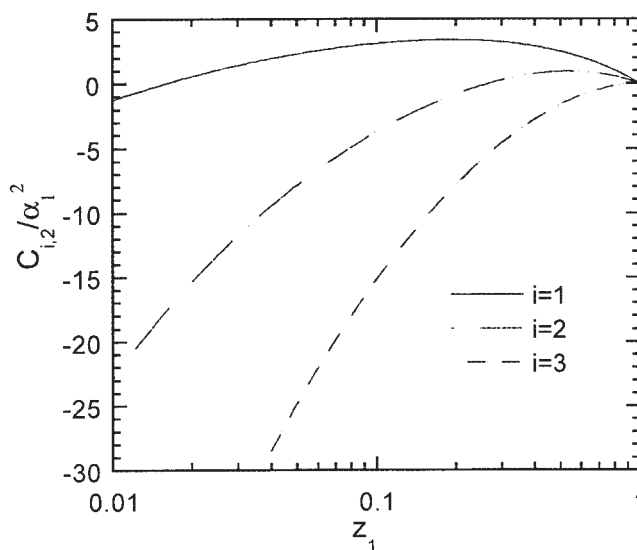


Figure 11. Functions $C_{i,2}$ (see Eq. 58) for $i=1$ to 3 and $b=1$, $d=-1/3$, $\alpha_1=10$.

initially (at $x=1$) take positive values, but as x tends to zero they diverge to plus and minus infinity in an alternating manner. The function $C_{i,2}$ for i up to three is shown in Figure 11. It is obvious that as i increases, the functions tend faster to negative values and diverge at a higher rate. In a sense, as i increases the functions $C_{i,k}$ are amplified. The divergence of the functions $C_{i,k}(x)$ is clear from the analytical solution (Eqs. 38–40) for the case $b=d$ for which $C_{i,k}(x)$ for d negative diverges at $x=0$ as $x^{d(k-1)}$. This analytical solution permits the extensive study of the convergence properties of series Eq. 37 for d negative.

It is well known that for breakage rate exponent $b<0$, particles with zero size but finite mass appear. This is the so-called shattering phenomenon (McGrady and Ziff, 1987). It is possible that a negative diffusivity exponent ($d<0$) leads to the instantaneous deposition of these zero size particles preventing in this way the shattering phenomenon. The influence of the diffusion and deposition of particles on the appearance of shattering is an issue that deserves further study.

Conclusions

This work deals with a population balance which combines diffusion with respect to external (spatial) coordinates and fragmentation, with respect to internal (particle volume) ones. Using the separation of variables technique, the problem is decomposed in spatial and temporal components. The spatial subproblem is well known from the theory of conduction and diffusion, whereas the temporal one resembles the (uniform in space) fragmentation equation with a deposition term. The latter subproblem can be solved using several iterative techniques which are reviewed and evaluated. On the basis of this analysis, general solutions of the diffusion-fragmentation equation, and the corresponding Green's functions are derived.

Explicit solutions are obtained for the particular case of equal size breakage and several results in one and two spatial dimensions are presented and discussed. In the case of binary random breakage the problem is transformed into a system of

Literature Cited

- Manuscript received March 20, 2003, revision received Nov. 12, 2003, and final revision received May 10, 2004.*